Visual Target Modulation of Functional Connectivity Networks Revealed by Self-Organizing Group ICA

◆ Human Brain Mapping 29:1450–1461 (2008) ◆

Visual Target Modulation of Functional Connectivity Networks Revealed by Self-Organizing Group ICA

Vincent van de Ven,[1]* Christoph Bledowski,[2] David Prvulovic,[3,4] Rainer Goebel,[1] Elia Formisano,[1] Francesco Di Salle,[1,5] David E.J. Linden,[6] and Fabrizio Esposito[1,7]

[1]*Department of Cognitive Neuroscience, Faculty of Psychology, University Maastricht, Maastricht, The Netherlands*
[2]*Institute of Medical Psychology, Johann Wolfgang Goethe University, Frankfurt am Main, Germany*
[3]*Brain Imaging Center, Johann Wolfgang Goethe University, Frankfurt am Main, Germany*
[4]*Laboratory for Neurophysiology and Neuroimaging, Department of Psychiatry, Johann Wolfgang Goethe University, Frankfurt am Main, Germany*
[5]*Department of Neurological Sciences, University of Pisa, Pisa, Italy*
[6]*School of Psychology, University of Wales, Bangor, United Kingdom*
[7]*Department of Neurological Sciences, University of Naples "Federico II", Naples, Italy*

Abstract: We applied a data-driven analysis based on self-organizing group independent component analysis (sogICA) to fMRI data from a three-stimulus visual oddball task. SogICA is particularly suited to the investigation of the underlying functional connectivity and does not rely on a predefined model of the experiment, which overcomes some of the limitations of hypothesis-driven analysis. Unlike most previous applications of ICA in functional imaging, our approach allows the analysis of the data at the group level, which is of particular interest in high order cognitive studies. SogICA is based on the hierarchical clustering of spatially similar independent components, derived from single subject decompositions. We identified four main clusters of components, centered on the posterior cingulate, bilateral insula, bilateral prefrontal cortex, and right posterior parietal and prefrontal cortex, consistently across all participants. Post hoc comparison of time courses revealed that insula, prefrontal cortex and right fronto-parietal components showed higher activity for targets than for distractors. Activation for distractors was higher in the posterior cingulate cortex, where deactivation was observed for targets. While our results conform to previous neuroimaging studies, they also complement conventional results by showing functional connectivity networks with unique contributions to the task that were consistent across subjects. SogICA can thus be used to probe functional networks of active cognitive tasks at the group-level and can provide additional insights to generate new hypotheses for further study. *Hum Brain Mapp 29:1450–1461, 2008.*

This article contains supplementary material available via the Internet at http://www.interscience.wiley.com/jpages/1065-9471/suppmat.

Contract grant sponsors: Alzheimer Research Initiative, Vigoni Programme of the German Academic Exchange Service (DAAD).

*Correspondence to: Vincent van de Ven, Department of Cognitive Neuroscience, Faculty of Psychology, University Maastricht, P.O. Box 616, 6200 MD, Maastricht, The Netherlands.
E-mail: v.vandeven@psychology.unimaas.nl

Received for publication 21 March 2006; Revised 19 June 2007; Accepted 14 June 2007
DOI: 10.1002/hbm.20479
Published online 7 November 2007 in Wiley InterScience (www.interscience.wiley.com).

Key words: fMRI; sogICA; posterior cingulate; prefrontal; group independent component analysis; oddball task; functional connectivity; posterior; parietal

INTRODUCTION

Functional brain imaging with functional magnetic resonance imaging (fMRI) or positron emission tomography (PET) provides the possibility to study neuronal brain responses during cognitive processes. Hypothesis-driven analyses like the general linear model (GLM) localize changes in signal according to task or stimulus presentation to the subjects. However, this analysis does not incorporate possible associations between regional timecourses, which may provide additional information about the functional specialization and integration of key brain areas [Friston, 1996]. Functional connectivity is operationally defined as the correlation between the timecourses of two spatially segregated areas [Friston, 1996], and is conceptually based on the notion that the brain comprises functionally specialized areas, which may interact with each other during task performance. Functional connectivity can be phrased as a multivariate problem, where the covariance matrix of a large number of regional or voxel timecourses is used as the starting point for the connectivity analysis. For example, Friston et al. [1993] used principal component analysis (PCA) to decompose the covariance matrix of task-related regional timecourses to estimate a set of orthogonal eigenimages that capture the degree of connectivity across the implicated brain areas. The neurophysiologically interesting connectivity patterns are typically found within the highest ranking principal components, according to component eigenvalues, and are characterized by spatial and temporal uncorrelatedness. An extension of this approach is the estimation of functional connectivity patterns using spatial independent component analysis [sICA: McKeown et al., 1998b]. As for PCA, components are decomposed without prior knowledge about the temporal profile of brain activity and the output maps of neurophysiologically interesting signals can be considered as maps of functional connectivity, where the component values of each map reflect the degree of connectivity [van de Ven et al., 2004; Yang and Rajapakse, 2004]. Differently from PCA, sICA assumes that the components are spatially independent, while the component timecourses are left free to be correlated to one another. Because of its more neurophysiologically plausible statistical model [Brown et al., 2001], sICA has proved successful in characterizing components of functional connectivity in a variety of situations [see McKeown et al., 2003, for a review], including complex naturalistic settings [Bartels and Zeki, 2004; Calhoun et al., 2002], auditory responses in schizophrenia [Calhoun et al., 2004; van de Ven et al., 2005] and during rest [Greicius et al., 2003; van de Ven et al., 2004].

While many sICA applications were inherently based on single-subject analyses, which may limit its use in studies of higher cognitive functions, there has been a recent increase in the development of multi-subject applications. Most of these developments focused on some combination of (preprocessed) functional data prior to ICA decomposition. Amongst the proposed approaches the concatenation of the data across subjects [Calhoun et al., 2001] rather than on time-points [Svensén et al., 2002] seems to provide the most reliable results, even when a component is not present in all subjects [Schmithorst and Holland, 2004]. A tensorial way of combining data-sets along a subject-specific new dimension of the analysis was also proposed [Beckmann and Smith, 2005]. However, an alternative approach combines components from single-subject decompositions *a posteriori*, but in a way that reduces investigator subjectivity in selecting and grouping the components. We propose that a cluster analysis that searches for similarity of components in the subject space might serve this purpose. Clustering of independent components can be achieved using component-descriptive parameters [van de Ven et al., 2002], such as spatial structure or distributions [Formisano et al., 2002], or task frequency [Moritz et al., 2003]. Esposito et al. [2005] suggested a different approach, where independent components of single-subject decompositions are grouped according to spatial, temporal, or combined spatio-temporal information using a self-organizing grouping procedure that is based on hierarchical cluster analysis [Himberg et al., 2004]. When performing ICA on a combined dataset, some preprocessing is applied to both the individual and the aggregate dataset [Calhoun et al., 2001]. This is not the same as grouping results after individual ICA decompositions. SogICA retains the individual ICA decompositions and uses a quantitative, similarity-based clustering procedure to group components across datasets. Furthermore, sogICA provides means for inspecting the intra-cluster degree of homogeneity between the components, which can be used to identify potential outliers and select strategies for subsequent improvement of the analyses.

The oddball paradigm and its variants are among the cognitive tasks that have been studied most extensively with fMRI and electrophysiology techniques. In this paradigm the subject is required to actively detect a target stimulus, which is infrequently and randomly presented within a train of frequent standard stimuli. FMRI studies demonstrated that target processing is associated with a cortical activity pattern comprising areas around the Sylvian fissure, including the supramarginal gyrus, inferior

and middle frontal gyrus and the insula, and midline areas, including the anterior and posterior cingulate and the supplementary motor area [see Linden, 2005, for a review]. The detection of rare, meaningful target events relies on the orchestration of several cognitive processes, including visual attention, working memory and stimulus categorization. This might be the reason why the described cortical activation pattern overlaps with those found in many other attention-demanding cognitive tasks, such as working memory or visual search [e.g., Corbetta and Shulman, 2002]. However, less is known about functional connectivity of these areas.

In this study, we applied sogICA [Esposito et al., 2005] to fMRI data obtained from a three-stimulus oddball paradigm that had already been studied with a GLM-based approach [Bledowski et al., 2004a]. The primary aim of this analysis was to determine functional connectivity patterns during the oddball task in an exploratory way. We furthermore expected that the time course analysis of the identified components would allow for a differentiation of target and distractor responses.

METHODS

Subjects

Functional imaging datasets of nine subjects were selected from an earlier study [Bledowski et al., 2004a]. The computational load forced a restriction upon the number of subjects that can be analyzed using sogICA. Therefore, we selected the nine best performing subjects from the original subject sample. They had correctly identified 85.9% of the targets (S.D. = 9.6%). The performances of all 13 subjects in the original sample were 82.6% ± 9.6% [Bledowski et al., 2004a]. The nine selected subjects comprised 6 males, and had a mean age (S.D.) of 29.4 (5.7) years. All were right-handed. None of the subjects had a history of neurological or psychiatric disorders. After the study was explained all subjects gave written informed consent to participate in the study. The study was approved by the local ethics committee.

Design

A three-stimulus visual oddball paradigm was used, where the stimulus categories comprised standard, target and distractor stimuli. The standard stimulus (blue circle, 1.53°) had a probability of occurrence of 0.9, while the target stimulus (blue circle, 1.38°), as well as the distractor stimulus (blue square, 1.36°), each had a probability of 0.05 to occur. The stimuli were presented to the subject in a random order, once every 2 s for 75 ms. The subject was required to respond via button press to the target stimulus only. Within each functional run 350 stimuli were presented.

Imaging Parameters

All functional and anatomical images were acquired using a 1.5 T Siemens Vision MR Tomograph (Siemens, Erlangen, Germany). The blood-oxygen-level dependent (BOLD) signal was measured using a gradient-echo echo-planar-imaging (EPI) sequence. For the functional images, 16 axial slices were obtained for each volume (repetition time [TR]/echo time [TE] = 2000/60 ms; voxel size = 3.6 × 3.6 × 5.0 mm^3; flip angle = 90°; field of view [FoV] = 230 × 230 mm^2), and each functional run contained 360 volumes. During the first 10 volumes no stimulus was presented, the onset of each proceeding volume triggered the onset of a stimulus. A 3D anatomical image was acquired in the same session for each subject (matrix size = 256 × 256; voxel size = 2.0 × 1.0 × 1.0 mm^3), which lasted about 5 min.

Preprocessing and Analysis

The first four volumes of each functional dataset were discarded because of saturation effects. The functional datasets were then corrected for inter-slice timing differences and scaled and resampled to Talairach space [Talairach and Tournoux, 1988] with a voxel size of 3 × 3 × 3 mm^3 using the BrainVoyager 4.8 analysis software (Brain Innovation, Maastricht, The Netherlands). The rescaled functional datasets were spatially smoothed using a Gaussian kernel of full-width-at-half-maximum [FWHM] of 6 mm, and temporally filtered using linear trend removal and high-pass filtering of 5 cycles/session (≈0.007 Hz). The anatomical images of all nine subjects were averaged, and a volume mask was created from this average image, which excluded voxels associated with matter outside of the brain and ventricle fluid. The remaining voxels were used for further analysis. This procedure was done to attenuate computational load, while keeping the subspaces of selected voxels for the analysis constant across subjects.

The preprocessed functional datasets were imported and analyzed in Matlab 6 (MathWorks, Mass), using the self-organizing grouping ICA (sogICA) software described elsewhere [see Supplementary information; Himberg et al., 2004; Esposito et al., 2005]. Briefly, the sogICA framework analyses individually decomposed datasets on a group level by clustering independent components in the subject space, using spatial correlation as similarity measure. This approach preserves subject specific information, and provides the investigator with a measure of spatial similarity of components of interest. Regardless of the cluster size, all subjects are considered for clustering and each subject contributes maximally one component to a cluster. Infomax, an ICA algorithm that is based on a gradient-descent learning algorithm [Bell and Sejnowski, 1995], was used to decompose each functional dataset into a set of 60 independent components. PCA was used to reduce the initial dimensions [equal to the number of timepoints; McKeown et al., 1998a] of the functional dataset to 60. The initial learning rate was set to 0.0001 and the batch size to 10. After decomposition, the map values of each component map were *Z*-scored [McKeown et al., 1998b].

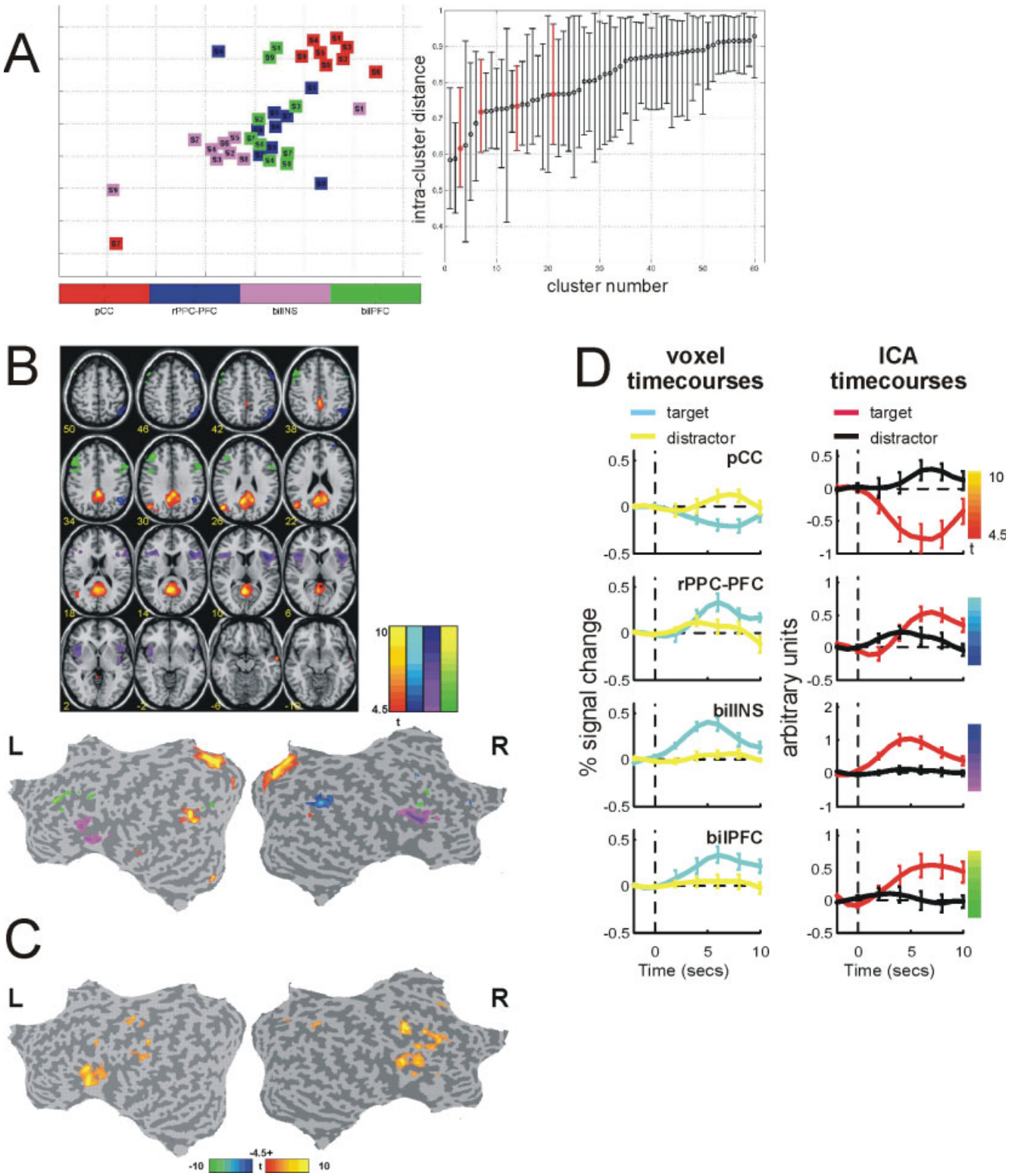

Figure 1.
(legend on page 1454)

For this study, the size of each cluster was set to nine components, where sogICA closed a cluster when it reached this size. Cluster "group" components were calculated as random effects maps using the cluster component members as input. The random effects statistic for each voxel was calculated as the mean ICA *Z*-value of that voxel across the individual maps divided by its standard error, resulting in a one-sample *t*-statistic. Statistical maps were then further corrected for multiple comparisons using cluster-size thresholding [Forman et al., 1995; Goebel et al., 2006]. In this method, for each statistical map the initial (uncorrected) voxel-level threshold was set at $P = 0.001$. Then, a whole-brain correction criterion based on the estimate of the map's spatial smoothness and on an iterative procedure (Monte Carlo simulation) for estimating cluster-level false-positive rates was applied. After 1,000 iterations the minimum cluster-size that yielded a cluster-level false-positive rate of 5% or less was used to threshold the statistical map, which was then superimposed on an anatomical brain template (Montreal Neurological Institute [MNI]). After sogICA was performed, we chose clusters of interest according to (1) the 10 clusters with the lowest mean intra-cluster distances, and (2) spatial templates of areas of interest, which included bilateral insula, inferior parietal cortex, dorsolateral prefrontal cortex, middle/inferior temporal cortex, posterior cingulate cortex, left sensorimotor cortex, and primary visual cortex (PVC) [Bledowski et al., 2004a; see Supplementary Information]. The search strategies were used independently in order to complement each other.

Group event-related averages for the clusters were calculated from the event-related averages of the individual components within each cluster. For each component map the voxel timecourses were extracted from voxels with positive suprathreshold *Z*-values. Voxel timecourses of the individual components for the target and distractor stimulus were transformed to percent BOLD signal change and averaged according to event type and presentation. For the target stimulus only correctly identified trials were used for event-related averaging. For each cluster, group event-related averages (and standard errors of the mean) were generated from the event-related averages of the individual components. For visualization the group event-related averages were interpolated to a resolution of 1 s.

RESULTS

The analysis of fMRI data with sogICA revealed four clusters of components that comprised suprathreshold voxel-clusters in cortical areas of interest. Figure 1 shows the clustering and group map results of these four clusters (voxel-level $t(8) = 4.5$, $P \leq 0.001$, corrected at the cluster-level 0.05). Table I lists the corresponding mean and range of the intra-cluster distances and the peak *t*-values of the group maps. The clusters of components are presented in the order of ascending mean intra-cluster distance, and the abbreviations refer to those in the figures and tables.

The first cluster of components comprised the posterior cingulate cortex (pCC), and anterior cingulate and bilateral inferior parietal cortex. These areas were found in all nine cluster members. The multi-dimensional scaling plot (Fig. 1A) indicated a potential outlier within the pCC cluster, that is, one cluster member (S7) is spatially displaced with respect to the other cluster members. Close inspection of this particular member's spatial layout revealed that, in addition to posterior cingulate and bilateral inferior parietal cortex, a large area of suprathreshold *Z*-values was located near the anterior cingulate cortex.

The second cluster (right posterior parietal and prefrontal cluster: rPPC-PFC) comprised suprathreshold voxels in right posterior parietal cortex and dorsolateral prefrontal cortex. All nine individual components showed a right lateralization of voxels with high *Z*-values.

The third cluster (bilateral insula: bilINS) comprised voxels in bilateral insular areas, frontal operculum, and inferior frontal gyri. Inspection of individual maps revealed additional areas of suprathreshold *Z*-values in inferior frontal and frontal medial areas in some, but not all, maps. Component maps of subjects S1 and S9, which had the largest intra-cluster distances (see Fig. 1A), contained similar areas but showed opposite lateralization of insula activity.

Figure 1.

Four clusters of interest selected from the sogICA results. (**A**) Multi-dimensional scaling plot (left) and range of the intra-cluster distribution of cluster members (right; minimum, mean and maximum). (**B**) Group spatial maps of the four clusters are superimposed on 16 transverse slices and flatmaps of the MNI brain ($t(8) = 4.5$; $P \leq 0.001$, corrected at the cluster-level of 0.05 with cluster-size thresholds of 306, 309, 292, and 292 mm^3, respectively). Colors of the spatial maps correspond to colors of the multi-dimensional scaling plot. (**C**) Hypothesis-driven random effects analysis of target and distractor processing ($t(8) = 4.5$; $P \leq 0.001$, corrected at the cluster-level 0.05; 405 mm^3). Only the results of target processing are shown, distractor processing did not reveal significant activity after cluster-level correction. Most cortical areas are found back in the selected clusters of components, while at the same time the components revealed additional spatiotemporal information about the activity and connectivity of cortical responses. (**D**) Group event-related averages of the target and distractor stimulus of the independent components. Left column: event-related averages obtained from each individual ICA map's suprathreshold voxels (units percent signal change). Right column: event-related averages obtained from the ICA-generated component timecourses (arbitrary units). pCC = posterior cingulate cluster; rPPC-PFC = right posterior parietal and prefrontal cluster; bilINS = bilateral insular cluster; bilPFC = bilateral prefrontal cluster.

TABLE I. Intra-cluster distances and talairach coordinates (x, y, z) of peak t-values (random effects) of cortical areas of the four clusters comprising nine components

	Intra-cluster distances					Coordinates (mm)				
COI	Mean	Min	Max	Area	Side	*x*	*y*	*z*	t_{max}	Size
pCC	0.62	0.51	0.79							
				pCC	L	−10	−56	24	24.5	19,964
				IPL	L	−46	−68	24	14.0	2,608
				MTG	R	59	−8	−12	10.6	328
rPPC-PFC	0.72	0.61	0.86							
				IPS	R	41	−53	33	8.9	4,734
					R	53	10	39	6.7	855
				SFG	R	26	7	57	11.0	942
					R	26	49	21	6.6	320
bilINS	0.73	0.61	0.85							
				IFG/FO/INS	R	38	10	9	10.1	6,779
				IFG	L	−34	19	15	8.5	5,288
				SFG	R	5	19	66	7.0	355
				pINS	L	−34	−17	−3	6.8	305
bilPFC	0.77	0.63	0.96							
				SFG/MFG	L	−37	31	30	8.0	4,299
				MFG	R	53	10	33	6.5	1,731

Size of voxel clusters is reported in number of anatomical voxels ($1 \times 1 \times 1$ mm^3). COI, cluster of interest; pCC, posterior cingulate cortex; SFG, superior frontal gyrus; MFG, middle frontal gyrus; IFG, inferior frontal gyrus; IPL, inferior parietal lobule; IPS, intra–parietal sulcus; MTG, middle temporal gyrus; INS, insula; FO, frontal operculum.

The fourth cluster (bilateral prefrontal cluster: bilPFC) comprised voxels in bilateral middle frontal gyrus, but also in parietal areas. Inspection of the individual maps indicated some variation in spatial location of suprathreshold voxel values. Two spatial components contained suprathreshold voxels in right posterior and dorsal frontal cortical areas. In the other components areas of suprathreshold voxels were found in both the left and right hemisphere. For one component, connectivity clusters were found in bilateral dorsal frontal areas, including frontal eye fields, but not in parietal areas.

Random effects group results using the GLM are shown in Figure 1C. Results were thresholded in a similar way as the ICA group maps ($t(8) = 4.5$; $P \leq 0.001$, corrected at the cluster-level 0.05). Most areas that showed increased activity for the target stimulus were also amongst the areas of the four selected sogICA clusters. In contrast to sogICA, the random effects analysis did not show significant activity changes for either stimulus in the posterior cingulate cortex. However, fixed effects analysis of the same data showed significantly decreased activity for the target, but not the distractor stimulus in this area (not shown). This discrepancy may be the result of low statistical power of the random effects analysis brought about by the small sample size (nine subjects), and shows that SogICA may complement conventional analysis approaches in the case of low statistical power.

Figure 1D depicts the group event-related averages and standard error of the mean for the target and distractor stimuli for the four clusters of components. The bilINS and bilPFC clusters showed event-related BOLD signal increases for the target stimulus, but not for the distractor stimulus. Right PPC–PFC showed a large increase of BOLD signal for the target stimulus and a small initial increase for the distractor stimulus. The pCC cluster showed a decrease of the BOLD signal for the target stimulus, and an increase of the BOLD signal for the distractor stimulus.

To verify that the selective averaging of the voxel timecourses yielded reliable results with respect to the ICA estimates, the component timecourses were averaged for each stimulus type (Fig. 1D). The event-related averages from voxel and component timecourses do not differ qualitatively. In all cases the target stimulus elicited the strongest response in comparison to the distractor stimulus; the pCC showed a large decrease of activity for the target stimulus while the other three clusters showed large increases of activity (Table II).

Different Contributions to Prefrontal Cortex

Three clusters of components showed a contribution of voxels in dorsolateral and ventrolateral prefrontal cortex. Examination of the voxels within these areas revealed different temporal profiles for processing of the target and distractor stimulus (Fig. 2; spatial coordinates of the areas are reported in Table I). Ventrolateral prefrontal areas, including left and right inferior frontal gyrus, showed a strong preference for the target stimulus, but not for the distractor stimulus. Dorsolateral prefrontal areas, including

TABLE II. Random-effects results of the time courses of the six selected clusters of components

			Predictors							
			Target			Distractor			Contrast	
N_{clu}		COI	$\bar{b}$	T	P	$\bar{b}$	t	P	T	P
9	VTC	pCC	−0.05	−1.6	0.161	0.02	0.9	0.399	−4.8	0.001
		rPPC	0.14	3.0	0.017	0.05	1.6	0.151	2.1	0.069
		bilINS	0.26	7.3	<0.001	0.03	1.3	0.223	6.1	<0.001
		lPFC	0.15	5.6	0.001	0.07	2.4	0.041	2.7	0.026
	ICtc	pCC	−0.15	−3.4	0.010	−0.01	−0.2	0.820	−0.2	0.012
		rPPC	0.17	5.9	<0.001	0.04	1.7	0.131	4.6	0.002
		bilINS	0.25	5.0	0.001	0.05	3.1	0.014	4.5	0.002
		lPFC	0.16	3.3	0.011	0.01	0.3	0.777	2.7	0.029
7	VTC	PVC	0.04	1.6	0.168	0.04	1.7	0.138	−0.1	0.934
		SMC	0.16	7.1	<0.001	0.02	0.8	0.462	5.2	0.002
	ICtc	PVC	−0.02	−0.9	0.410	0.03	1.3	0.235	−1.8	0.123
		SMC	0.11	3.0	0.024	−0.03	−1.4	0.225	4.6	0.004

Tests are significant at $P \leq 0.05$. Individual component time courses were standardized using Z-scoring. $\bar{b}$, mean beta value; VTC, voxel time courses; ICtc, independent component time courses; N_{clu}, number of components per cluster.

right superior and bilateral middle frontal gyrus, showed slightly increased activity for the distractor, as well as the target stimulus. These findings indicate that ICA is able to represent the heterogeneity of prefrontal activity.

Additional Clusters

We also searched for clusters of sensorimotor (SMC) and PVC. Components for these areas did not cluster well. Components of SMC were clustered into four different clusters, together with spatial maps that contained high Z-values in dorsal areas, but which were not likely related to the button press response. We therefore performed two additional clustering runs with cluster sizes of eight and seven subjects per cluster. Note that in these two additional runs the complete datasets were still used (i.e., 60 components × 9 subjects), and that each subject contributed maximally one component to each cluster, but clusters including less subjects (i.e., 8 and 7) were allowed. With this reduced cluster size, clustering for these areas improved with decreasing cluster size (i.e., relatively small minimum, mean, and maximum intra-cluster distances, see Fig. 3A and Table III). Figure 3B and C show the spatial maps and event-related averages of SMC and PVC (cluster size = 7), and Table III lists the spatial coordinates of suprathreshold voxel clusters. Left SMC revealed increased activity for the target stimulus, reflecting the button presses associated with target detection. PVC showed no change from baseline for either of the stimulus categories (see Table II). Figure S2 of the supplementary information provides a schematic overview of the results of decreased cluster sizes for the SMC and PVC clusters.

DISCUSSION

We performed a data-driven analysis of the functional imaging data of a three-stimulus oddball task for nine subjects using the sogICA framework to interpret the results at group level. The sogICA results provided functional connectivity components of functional networks involved in an attention-demanding cognitive task. More precisely, sogICA grouped the decompositions of individual datasets into clusters, where each subject contributed maximally one component to each cluster. Four clusters of interest of spatial component maps were found (pCC, rPPC-PFC, biINS, and bilPFC). When clustering the components using a smaller cluster size two additional clusters were obtained (PVC and SMC).

Posterior Cingulate Cluster

The posterior cingulate cluster (pCC) cluster, which contained anterior and posterior cingulate and bilateral inferior parietal cortex, corresponds well to the "default mode network" (DMN) [Greicius et al., 2003; Raichle et al., 2001]. DMN areas have been found during rest [Fox et al., 2005; van de Ven et al., 2004], and their activity is inversely correlated with that in frontal and parietal cortex during active cognitive tasks [Shulman et al., 1997]. The event-related time courses in the present study showed increased activity for the distractor, and decreased activity for the target stimulus. The frequent standard stimuli, which were very similar to the targets, required an ongoing goal-directed behavior. The task-relevant target stimulus demanded additional processing resources, which was reflected in suppression of the DMN, whereas the task-irrelevant distractor stimuli, although drawing attentional resources, did not demand goal-directed processes.

Right Posterior Parietal and Prefrontal Cluster

In all subjects the decompositions resulted in a component of right PPC and right middle and superior frontal gyrus. A dissociation of right and left fronto-parietal areas

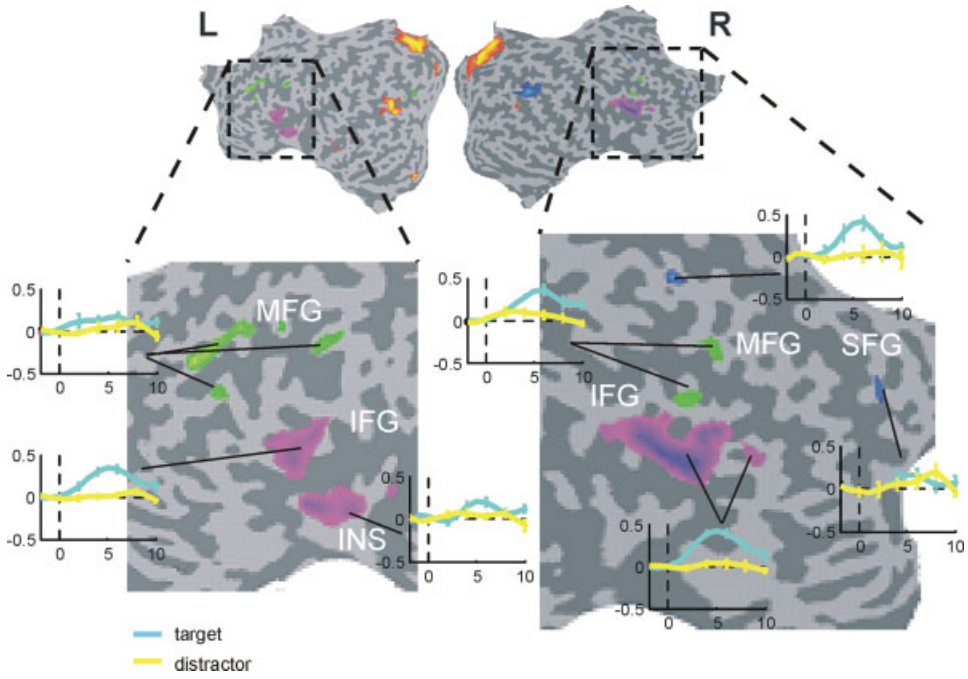

Figure 2.
Contribution of different component clusters to prefrontal cortex. Parts of left and right prefrontal cortex within the MNI flatmaps are enlarged. Group event-related averages of the voxel timecourses are shown next to the corresponding voxel cluster. The figure shows that prefrontal cortex comprises spatial contributions from different independent components with different temporal profiles for the target and distractor stimulus. Flatmap colors correspond to cluster colors of Figure 1. IFG = inferior frontal gyrus; MFG = middle frontal gyrus; SFG = superior frontal gyrus; INS = insula.

was also observed in an fMRI study of functional connectivity during rest [van de Ven et al., 2004]. The prominence of the rPPC-PFC cluster in the present decomposition may indicate a differential contribution of the right hemisphere to visual attention [Coull et al., 1998; Lawrence et al. 2003; Muggleton et al., 2003; O'Shea et al., 2004] and conforms to the postulated ventral right fronto-parietal attention network [Corbetta and Shulman, 2002]. It has been suggested that this network is recruited for the detection of behaviorally relevant and unexpected stimuli. During the oddball task rare stimuli (target and distractor) occur randomly in a sequence of standard stimuli. The saliency of the rare events is reflected in an initial increase of activity in the respective parietal and frontal areas. Further processing, however, may then only be allocated to those stimuli identified as targets, resulting in a further increase of activity. This interpretation is supported by the initial increase of

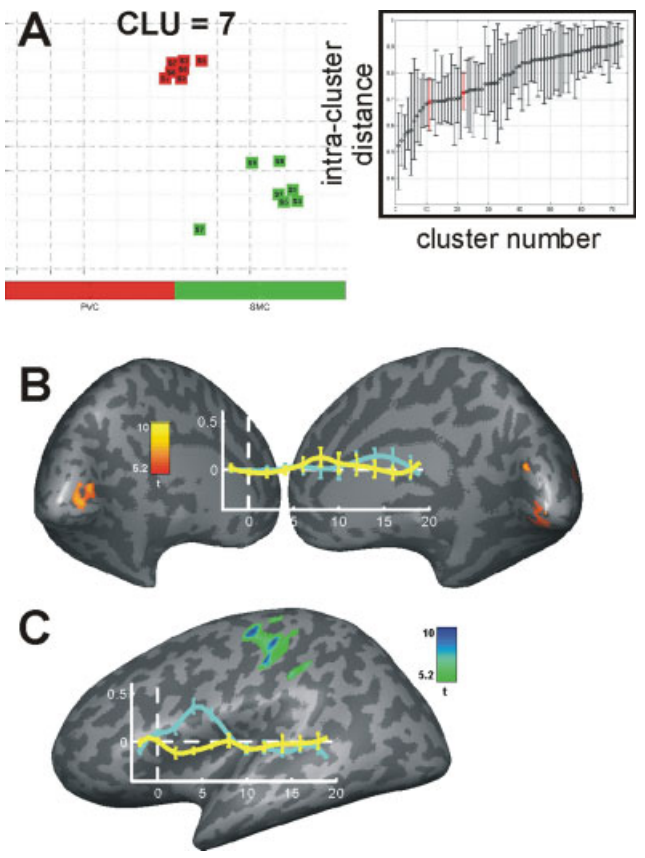

Figure 3.
Primary visual (PVC) and sensorimotor clusters (SMC). (**A**) Multi-dimensional scaling plot (left) and range of the intra-cluster distribution of cluster members (minimum, mean and maximum). (**B** and **C**) Spatial group map and group event-related averages of the primary visual (B) and sensorimotor cortex cluster (C). Maps were thresholded at $t(6) = 5.2$ ($P \leq 0.001$, corrected at the cluster-level 0.05; 238 and 194 mm^3, respectively).

TABLE III. Intra-cluster distances and talairach coordinates (*x*, *y*, *z*) of peak *t*-values (random effects) of cortical areas of SMC and PVC clusters

	Intra-cluster distances					Coordinates (mm)				
COI	Mean	Min	Max	Area	Side	*x*	*y*	*z*	t_{max}	Size
PVC	0.69	0.58	0.78							
				LG	L	−15	−73	1	10.9	6,516
						−16	−65	−15	6.8	305
				Cu/CalcF	R	5	−77	18	13.6	441
SMC	0.72	0.66	0.80							
				PostCG	L	−55	−23	48	18.5	233
					R	56	−23	48	9.9	23
				Cerebellum	R	23	−41	−21	9.8	16

Mean and range (minimum–maximum) intra-cluster distances are reported for each cluster. Cluster size, 7 components; LG, lingual gyrus; Cu/CalcF, Cuneus/Calcarine fissure; PostCG, postcentral gyrus.

activity of the event-related time-courses of both types of rare stimuli, followed by a further increase for the target stimulus.

Bilateral Insular Cluster and Bilateral Prefrontal Clusters

The prefrontal cortex has been traditionally assumed to play a cue role in higher cognitive processes like working memory, selective attention, and target detection [Corbetta and Shulman, 2002; Curtis and D'Esposito, 2003; Linden, 2005]. However, several studies indicated the need for a functional separation within this network. For example, the dorsolateral prefrontal cortex has been associated with monitoring processes or rule representations [Passingham and Sakai, 2004; Ranganath and D'Esposito, 2005], whereas the more ventral part of the prefrontal cortex areas might represent memory retrieval processes [Bledowski et al., 2006; Petrides, 2002]. In our data set, the sogICA decomposed the prefrontal areas into two independent components of bilateral clusters bilPFC (including MFG, IFG, and also IPS) and bilINS (including IFG and anterior insula), which supports distinct functional systems within the prefrontal cortex. The analysis of event-related BOLD-signal changes indicated that both frontal components were involved in the processing of the target stimulus. A successful detection of targets required an orchestration of processes like monitoring, comparison of the memory template with incoming stimulus representation and response decision, which would explain the need for both DLPFC and VLPFC involvement.

Primary Visual Cluster and Sensorimotor Cluster

The remaining two clusters (SMC and PVC) showed a higher degree of spatial variability across the cluster members in comparison to the "cognitive" components, as reflected by the relatively high intra-cluster distances. When the clustering of components was performed with smaller cluster sizes, the clustering for SMC and PVC improved markedly. The initial failure of the sogICA framework to cluster the SMC components may have been due to either an overall higher inter-subject variability of the spatial patterns or the presence of "interfering" components with high *Z*-values in similar dorsal areas. We were notified of the presence of interfering components by the same cluster plot provided by the sogICA framework and observed how these components, which were extracted only from a small subset of the subjects, expressed different and possibly competitive neurophysiological processes. A deeper investigation into the individual pattern revealed functional networks with a different global architecture, although they were locally overlapping with the cluster representative components.

The cluster comprising PVC did not show increased activity for either stimulus types. This can be explained by the fact that a visual stimulus was presented during each measured functional volume. At the same time, the lack of differential activity shows that the PVC does not represent the behavioral relevance of the stimulus.

Cognitive Functional Networks

The visual oddball task has been used to investigate brain activity related to attention, memory, and categorization processes, and conventional hypothesis-driven approaches have shown a widespread cortical activity including frontal, parietal, and temporal areas as a function of the detection of odd, meaningful target events [Corbetta and Shulman, 2002; Linden, 2005]. However, less is known about the brain dynamics of ongoing activity during the oddball task and the modulation of these brain dynamics by the processing of a target event. Using a correlation analysis of ongoing spontaneous activity Fox et al. [2006] showed brain dynamics in the absence of a cognitive task, which could be parcellated into a ventral and a dorsal functional subsystem, and which overlapped with brain areas of attentional processes [Corbetta and Shulman, 2002].

Our study provides an alternative approach to analysing and interpreting the brain dynamics during this complex

cognitive task. While sogICA replicated to a large extent the findings of the hypothesis-driven analysis [Bledowski et al., 2004a], it also provided a separation of several functional connectivity networks that contributed uniquely, but consistently across subjects to the cognitive task. Moreover, we observed that the presentation of a target event elicited an activity increase in the three frontal and fronto-parietal networks (rPPC-PFC, bilINS, and bilPFC), and a decrease of the pCC network. We suggest that the rPPC-PFC network corresponds to the proposed stimulus-driven attentional system [Corbetta and Shulman, 2002; Fox et al. 2006], responsible for the detection and reorientation of the attentional resources toward the potentially relevant event, whereas the activity in the bilINS network reflects the cognitive capacity invested in memory retrieval in order to decide if the detected events match the internal representation of the target category [Bledowski et al., 2006]. In contrast, the bilPFC network, although modulated by the target event, can be associated with ongoing monitoring processes as recently proposed by Fox et al. [2006]. This view is supported by the small contribution of the PFC electric source activities to the target-related ERP signal [Bledowski et al., 2004b, 2006].

Methodological Considerations

The presented spatial independent components can be interpreted as maps of functional connectivity [van de Ven et al., 2004; Yang and Rajapakse, 2004], because the maps indicate a high amount of shared information on a time-point-by-timepoint basis. These connectivity maps may provide more information about the degree of functional coupling with respect to connectivity maps derived from PCA, where the spatial components are constrained by orthogonality of the timecourses. Spatial independence is a much stronger statistical criterion [McKeown et al., 1998a,b] and ICA maps can be considered as higher-order connectivity maps [Yang and Rajapakse, 2004]. Data-driven component-based techniques such as PCA and ICA complement interregional correlation analysis to investigate whole-brain functional connectivity because they do not require the specification of location and extension of regions of interest (the "seed voxels" of correlation analysis) in advance [Greicius et al., 2004; Ma et al., 2007]. However, the interpretation of the presentation of different brain areas into different ICA components in terms of the underlying neural mechanisms remains difficult, which is in part owed to the indirect measurement of neuronal activity in fMRI.

Components may be further analyzed for patterns of effective connectivity [Friston, 1996] by considering the temporal relations within and between components. Indeed, a growing list of effective connectivity analyses may be combined with ICA in future studies [c.f., Formisano and Goebel, 2003; Londei et al., 2006; Shimizu et al., 2006].

It is imperative that spatial ICA results can be interpreted on a group level, which allows inference and generalization to the population of interesting spatial modes. Multi-subject spatial ICA has received increased interest in the literature, where different strategies for grouping and analysis have been suggested [Beckmann and Smith, 2005; Calhoun et al., 2001; Esposito et al., 2005; Svensén et al., 2002]. SogICA performs temporal dimension reduction and ICA decomposition of each subject's time-series and sequentially clusters spatially consistent components across subjects. Although computationally more demanding than other aggregrate approaches, the sogICA solution keeps to a minimum possible between-subject variance effects in the data reduction and component extraction stages. The consequent limitation in the number of subjects will be addressed in future works by replicating the subject-level clustering procedure in a hierarchical fashion and by combining sogICA with other aggregate techniques.

CONCLUSIONS

In conclusion, sogICA revealed a small number of specific functional networks, with unique temporal profiles for target or distractor stimulus processing, which showed a high consistency across subjects. While the pCC cluster, which included other areas of the DMN as well, showed a deactivation for targets but not for distractors, higher responses for targets were observed in the three frontal and fronto-parietal networks. These findings suggest that the cognitive task of target detection recruits a set of specific functional networks that involve frontal and parietal brain areas.

ACKNOWLEDGMENTS

The authors thank Adriana Aragri for helpful discussions.

REFERENCES

Bartels A, Zeki S (2004): Brain dynamics during natural viewing conditions—A new guide for mapping connectivity in vivo. Neuroimage 24:339–349.

Beckmann CF, Smith SM (2005): Tensorial extensions of independent component analysis for multisubject fMRI analysis. Neuroimage 25:294–311.

Bell AJ, Sejnowski TJ (1995): An information maximisation approach to blind separation and blind deconvolution. Neural Comput 7:1129–1159.

Bledowski C, Prvulovic D, Goebel R, Zanella FE, Linden DEJ (2004a): Attentional systems in target and distractor processing: A combined ERP and fMRI study. Neuroimage 22:530–540.

Bledowski C, Prvulovic D, Hoechstetter K, Scherg M, Wibral M, Goebel R, Linden DE (2004b): Localizing P300 generators in visual target and distractor processing: A combined event-related potential and functional magnetic resonance imaging study. J Neurosci 24:9353–9360.

Bledowski C, Cohen Kadosh K, Wibral M, Rahm B, Bittner RA, Hoechstetter K, Scherg M, Maurer K, Goebel R, Linden DEJ (2006): Mental chronometry of working memory retrieval: A combined fMRI and ERP approach. J Neurosci 26:821–829.

Brown GD, Yamada S, Sejnowski TJ (2001): Independent component analysis at the neural cocktail party. Trends Neurosci 24:54–63.

Calhoun VD, Adali T, Pearlson GD, Pekar JJ (2001): A method for making group inferences from functional MRI using independent component analysis. Hum Brain Mapp 14:140–151.

Calhoun VD, Pekar JJ, McGinty VB, Adali T, Watson TD, Pearlson GD (2002): Different activation dynamics in multiple neural systems during simulated driving. Hum Brain Mapp 16:158–167.

Calhoun VD, Kiehl KA, Liddle PF, Pearlson GD (2004): Aberrant localization of synchronous hemodynamic activity in auditory cortex reliably characterizes schizophrenia. Biol Psychiatry 55:842–849.

Corbetta M, Shulman GL (2002): Control of goal-directed and stimulus-driven attention in the brain. Nat Rev Neurosci 3:201–215.

Coull JT, Frackowiak RSJ, Frith CD (1998): Monitoring for target objects: Activation of right frontal and parietal cortices with increasing time on task. Neuropsychologia 36:1325–1334.

Curtis CE, D'Esposito M (2003): Persistent activity in the prefrontal cortex during working memory. Trends Cogn Sci 7:415–423.

Esposito F, Scarabino T, Hyvärinen A, Himberg J, Formisano E, Comani S, Tedeschi G, Goebel R, Seifritz E, Di Salle F (2005): Independent component analysis of fMRI group studies by self-organizing clustering. Neuroimage 25:193–205.

Forman SD, Cohen JD, Fitzgerald M, Eddy WF, Mintun MA, Noll DC (1995): Improved assessment of significant activation in functional magnetic resonance imaging (fMRI): Use of a cluster-size threshold. Magn Reson Med 33:636–647.

Formisano E, Goebel R (2003): Tracking cognitive processes with functional MRI mental chronometry. Curr Opin Neurobiol 13:174–181.

Formisano E, Esposito F, Kriegeskorte N, Tedeschi G, Di Salle F, Goebel R (2002): Spatial independent component analysis of functional magnetic resonance imaging time series: Characterization of the cortical components. Neurocomputing 49:241–254.

Fox MD, Snyder AZ, Vincent JL, Corbetta M, van Essen DC, Raichle ME (2005): The human brain is intrinsically organized into dynamic, anticorrelated functional networks. Proc Natl Acad Sci USA 102:9673–9678.

Fox MD, Corbetta M, Snyder AZ, Vincent JL, Raichle ME (2006): Spontaneous neuronal activity distinguishes human dorsal and ventral attention systems. Proc Natl Acad Sci USA 103:10046–10051.

Friston KJ (1996): Statistical parametric mapping and other analyses of functional imaging data. In: Toga AW, Mazziotta JC, editors. Brain Mapping: The methods. San Diego: Academic Press. pp 363–396.

Friston KJ, Frith CD, Liddle PF, Frackowiak RSJ (1993): Functional connectivity: The principal component analysis of large (PET) data sets. J Cereb Blood Flow Metab 13:5–14.

Goebel R, Esposito F, Formisano E (2006): Analysis of functional image analysis contest (FIAC) data with BrainVoyager QX: From single-subject to cortically aligned group general linear model analysis and self-organizing group independent component analysis. Hum Brain Mapp 27:392–401.

Greicius MD, Krasnow B, Reiss AL, Menon V (2003): Functional connectivity in the resting brain: A network analysis of the default mode hypothesis. Proc Natl Acad Sci USA 100:253–258.

Greicius MD, Srivastava G, Reiss AL, Menon V (2004): Default-mode network activity distinguishes Alzheimer's disease from healthy aging: Evidence from functional MRI. Proc Natl Acad Sci USA 101:4637–4642.

Himberg J, Hyvärinen A, Esposito F (2004): Validating the independent components of neuroimaging time series via clustering and visualization. Neuroimage 22:1214–1222.

Lawrence NS, Ross TJ, Hoffmann R, Garavan H, Stein EA (2003): Multiple neuronal networks mediate sustained attention. J Cogn Neurosci 15:1028–1038.

Linden DEJ (2005): The P300: Where in the brain is it produced and what does it tell us? Neuroscientist 11:563–576.

Londei A, D'Ausilio A, Basso D, Belardinelli MO (2006): A new method for detecting causality in fMRI data of cognitive processing. Cogn Process 7:42–52.

Ma L, Wang B, Chen X, Xiong J (2007): Detecting functional connectivity in the resting brain: A comparison between ICA and CCA. Magn Reson Imag 25:47–56.

McKeown MJ, Jung T-P, Makeig S, Brown G, Kindermann SS, Lee T-W, Sejnowski TJ (1998a): Spatially independent activity patterns in functional MRI data during the Stroop color-naming task. Proc Natl Acad Sci USA 95:803–810.

McKeown MJ, Makeig S, Brown G, Jung T-P, Kindermann SS, Bell AJ, Sejnowski TJ (1998b): Analysis of fMRI data by blind separation into independent spatial components. Hum Brain Mapp 6:160–188.

McKeown MJ, Hansen LK, Sejnowski TJ (2003): Independent component analysis of functional MRI: What is signal and what is noise? Curr Opin Neurobiol 13:620–629.

Moritz CH, Rogers BP, Meyerand ME (2003): Power spectrum ranked independent component analysis of a periodic fMRI complex motor paradigm. Hum Brain Mapp 18:111–122.

Muggleton NG, Juan C-H, Cowey A, Walsh V (2003): Human frontal eye fields and visual search. J Neurophysiol 89:3340–3343.

O'Shea J, Muggleton NG, Cowey A, Walsh V (2004): Timing of target discrimination in human frontal eye fields. J Cogn Neurosci 16:1060–1067.

Passingham D, Sakai K (2004): The prefrontal cortex and working memory: Physiology and brain imaging. Curr Opin Neurobiol 14:163–168.

Petrides M (2002): The mid-ventrolateral prefrontal cortex and active mnemonic retrieval. Neurobiol Learn Mem 78:528–538.

Raichle ME, MacLeod AM, Snyder AZ, Powers WJ, Gusnard DA, Shulman GL (2001): A default mode of brain function. Proc Natl Acad Sci USA 98:676–682.

Ranganath C, D'Esposito M (2005): Directing the mind's eye: Prefrontal, inferior and medial temporal mechanisms for visual working memory. Curr Opin Neurobiol 15:175–182.

Schmithorst VJ, Holland SK (2004): Comparison of three methods of generating group statistical inferences from independent component analysis of functional magnetic resonance imaging data. J Magn Reson Imaging 19:365–368.

Shimizu S, Hyvärinen A, Hoyer PO, Kano Y (2006): Finding a causal ordering via independent component analysis. Comput Stat Data Anal 50:3278–3293.

Shulman GL, Fiez JA, Corbetta M, Buckner RL, Miezin FM, Raichle ME, Petersen SE (1997): Common blood flow changes across visual tasks. II. Decreases in cerebral cortex. J Cogn Neurosci 9:648–663.

Svensén M, Kruggel F, Benali H (2002): ICA of fMRI group study data. Neuroimage 16:551–563.

Talairach J, Tournoux P (1988): Coplanar Stereotaxic Atlas of the Human Brain. New York: Thieme Medical.

van de Ven VG, Sack AT, Linden DEJ, Formisano E (2002): Independent Component Analysis of fMRI Data: Identifying Components of Interest. Orlando, Florida, USA: Society for Neuroscience Abstract. pp 506, 16.

van de Ven VG, Formisano E, Prvulovic D, Roeder CH, Linden DEJ (2004): Functional connectivity as revealed by spatial independent component analysis of fMRI measurements during rest. Hum Brain Mapp 22:165–178.

van de Ven VG, Formisano E, Röder CH, Prvulovic D, Bittner RA, Dietz MG, Hubl D, Dierks T, Federspiel A, Esposito F, Di Salle F, Jansma B, Goebel R, Linden DE (2005): The spatiotemporal pattern of auditory cortical responses during verbal hallucinations. Neuroimage 27:644–655.

Yang K, Rajapakse JC (2004): ICA gives higher-order functional connectivity of brain. Neural Information Processing. Lett Rev 2:27–32.